

# Sub-100 nm lithography using ultrashort wavelength of surface plasmons

W. Srituravanich, N. Fang, S. Durant, M. Ambati, C. Sun, and X. Zhang<sup>a)</sup>

Center for Scalable and Integrated Nanomanufacturing, University of California at Los Angeles, Los Angeles, California 90095-1597

(Received 4 June 2004; accepted 4 October 2004; published 14 December 2004)

The development of a nanolithography technique utilizing ultrashort wavelength of surface plasmons (SPs) is presented in this article. The mask consists of silver thin film perforated with two-dimensional hole arrays exhibiting superior confinement due to SPs with a wavelength equal to  $\frac{1}{4}$  of that of the illuminating light (365 nm). This short wavelength of SPs can confine the field on an area much smaller compared to the excitation light wavelength, leading to the higher resolution lithography than conventional photolithography methods. Finite-difference time-domain simulations show significantly enhanced electric field and tight confinement of the near-field profile obtained from silver plasmonic masks, where features as small as 30 nm can be resolved. Furthermore, the lithography experiments have been performed with demonstration of sub-100 nm spatial resolution. © 2004 American Vacuum Society. [DOI: 10.1116/1.1823437]

## I. INTRODUCTION

The rapid growth of nanotechnology is stimulated by the advancement of nanolithography. Methods such as optical contact lithography,<sup>1-4</sup> electron-beam lithography,<sup>5</sup> imprint lithography,<sup>6-8</sup> scanning probe lithography,<sup>9,10</sup> and dip-pen lithography<sup>11,12</sup> have been developed to fabricate nanostructures. Among them, imprint lithography and optical lithography are of particular interest due to the high throughput for mass fabrication. Imprint lithography can generate nanometer-scale features by stamping a template on a thin polymer film. However, the requirement of high aspect ratio masks, and the leveling of the imprint template and the substrate during the printing process in order to achieve uniform imprint results are major concerns of this method.<sup>6-8</sup> On the other hand, optical lithography has been a major fabrication method in semiconductor industries over the past several decades. Recent progress in optical contact lithography<sup>1-4</sup> utilizing the near-field promises sub-100 nm resolution at low cost. However, there are several critical concerns, such as extremely low transmission through the apertures, reduced contrast associated with the distance away from the mask, and poor field confinement due to the spreading out of the field. Recently, we demonstrated a high density lithography using surface plasmon (SP) enhanced transmission through subwavelength hole array.<sup>13</sup> A two-dimensional (2D) dot array pattern with feature size of 90 nm on a 170 nm period has been obtained using an exposure radiation of 365 nm wavelength. However, the pattern size seems to be larger than the design mask (40 nm aperture size) due to poor field confinement. In this article, we utilize ultrashort wavelength of SPs in order to further confine the plasmonic field on an area much smaller compared to the excitation light wavelength, leading to the higher resolution than those were achieved by conventional photolithography methods. A high-resolution UV nanolithography using 2D silver plasmonic

masks (the configuration of the SP optical lithography is shown in Fig. 1) is demonstrated. The advantages of this method are superior confinement of the near field and a strongly enhanced field owing to the much shorter wavelength of SPs.

The potential of using SPs to manipulate light in the sub-wavelength spaces opens up a multitude of new possibilities for subwavelength lithography, data storage, microscopy, and biophotonics.<sup>14</sup> The recent discovery of extraordinary transmission through metal films perforated with a periodic array of subwavelength holes has stimulated extensive interest in SPs within the scientific community.<sup>15-19</sup> This unusual enhancement is attributed to the excitation of SPs on the metal surface, which dramatically enhances light transmission through subwavelength apertures. The interaction of light and SPs is described by the SP dispersion relation (the frequency-dependent SP wave vector  $k_{SP}$ ) in Eq. (1),<sup>20</sup> as

$$k_{SP} = k_0 \sqrt{\frac{\epsilon_d \epsilon_m}{\epsilon_d + \epsilon_m}}, \quad (1)$$

where  $k_0$  is the wave vector of light in vacuum, and  $\epsilon_m$  and  $\epsilon_d$  are dielectric constants of a metal and a surrounding dielectric material, respectively. According to the SP dispersion curve, the wavelength of the excited SPs can become much shorter compared to the wavelength of the excitation light; therefore, it allows one to produce smaller features in the lithography process. This SP wavelength is analogous to light traveling in a very high refractive index medium. Generally, light cannot excite SPs on the metal surface directly due to the momentum mismatch between the light waves and the SP waves. The conversion between light and SPs can only be achieved with the existence of momentum matching elements, which typically consists of rough surface, grating coupler or attenuated total reflection coupler. For instance, a 2D square array of holes can be treated as a 2D grating coupler. By selecting a proper periodicity of hole array, and a proper dielectric constant of the medium surrounding the metal substrate, light can excite SP waves on the incident

<sup>a)</sup>Author to whom correspondence should be addressed; electronic mail: xiang@seas.ucla.edu

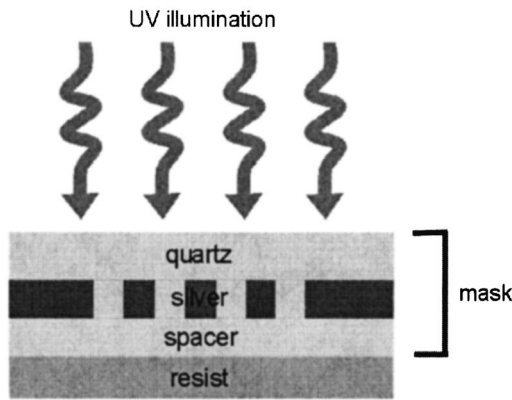


FIG. 1. Schematic drawing of the SP optical lithography. FIB is used to fabricate 2D hole array on silver substrate.

side, and for thick metal case, these SP waves can be resonantly coupled through the periodic hole array to the other side of the metal.<sup>15,17</sup> If the dielectric constant of the dielectric layers match on both sides of the metal layer, the SP waves on the exit plane scattered on the hole array will be converted back into the light waves. In the case of a normal incident light on a 2D hole array, the light wavelengths which excite the SP resonance mode are approximated by<sup>17</sup>

$$\lambda(i,j) = \frac{a}{\sqrt{i^2 + j^2}} \sqrt{\frac{\epsilon_d \epsilon_m}{\epsilon_d + \epsilon_m}}, \quad (2)$$

where  $\lambda$  is the light wavelength in vacuum,  $a$  is the hole array period, and  $i$  and  $j$  are mode indices.

## II. SAMPLE DESIGN

In order to utilize ultrashort wavelength of SPs, the SP dispersion curves of four highly conductive metals (silver, aluminum, gold, and copper) are calculated using Eq. (1). As shown in Fig. 2, silver (Ag) exhibits the largest SP wave vector (real part of  $k_{SP}$ ) at a wavelength of 365 nm (*i*-line) when surrounded by a dielectric material (refractive index  $n=1.52$ ). The dielectric constants of metals are taken from Ref. 21. The SP wavelength in this case is equivalent to  $\lambda/4$ , where  $\lambda$  is the wavelength of light in vacuum. The SP wavelength represents the maximally enhanced field that can be excited on the metal surface that approximates the optimal pattern resolution. At such short SP wavelength, the features of 30 nm (60 nm periodicity) can be resolved as we obtained by sweeping the periodicity in numerical simulation. To this end, we performed a number of numerical simulations on plasmonic mask, which consists of an array of circular holes in the silver film, to explore the transmitted electric field and confinement at this wavelength. The three-dimensional simulations were done by using a commercial finite-difference time-domain (FDTD) software (Microwave Studio) and the results have been shown by their cross-sectional images at the center of the holes (Fig 3). Under the plane wave illumination ( $\lambda=365$  nm) with the incident electric field linearly polarized along the  $x$  axis as shown in Fig. 3(a) and an amplitude of 1 V/m, the electric field transmitted through silver

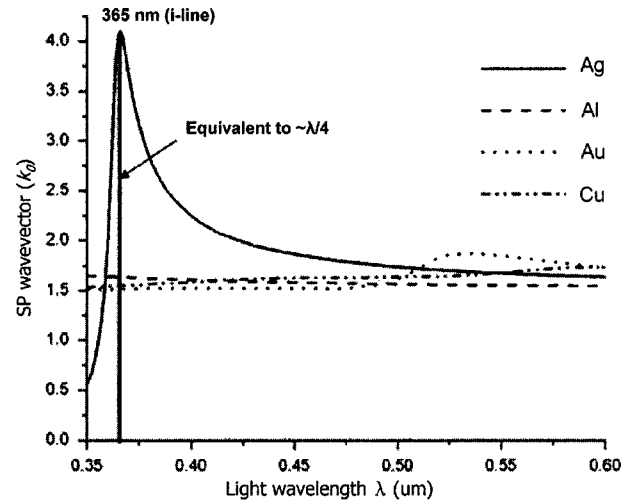


FIG. 2. SP wave vector of highly conductive metals (Ag, Al, Au, and Cu) surrounded by a dielectric material with the refractive index  $n=1.52$ . Silver (Ag) exhibits the largest SP wave vector ( $\sim 4k_0$ ) at a wavelength of 365 nm. The SP wavelength in this case is equivalent to  $\lambda/4$ , where  $\lambda$  is the wavelength of light in vacuum.

hole array [Fig. 3(a)] exhibits significant enhancement of the field strength and tight confinement of the field distribution compared with that of the aluminum hole array [Fig. 3(b)]. This offers the opportunity to further extend the resolution limit of the plasmonic lithography. The hole diameter, hole array periodicity, and silver layer thickness are 60, 120, and 40 nm, respectively. The refractive index  $n$  of the background material is 1.52. The refractive indices of Ag and Al are  $0.218+1.596i$  and  $0.407+4.426i$ , respectively, as taken from Ref. 21. The grid size is  $\lambda/30$ , where  $\lambda$  is the wavelength of illumination light (365 nm). The convergence criterion was set at  $-80$  dB, where the pulse incident field propagates through the sample and residue energy is below  $-80$  dB. Figure 3(c) shows the electric field amplitude of the simulation result in Fig. 3(a) as a function of distance  $z$  below the mask. It is noted that the electric field is concentrated on the metal area rather than the hole area. In contrast to the common wisdom that a skin depth of silver is about 20 nm at optical wavelength, to our understanding, the metal film is thin enough to allow the coupling of SPs between the top and bottom surfaces due to multiple reflections of waves at the interface. This coupling leads to the electric field at the exit plane being enhanced up to 3.5 times compared with the incident field. Furthermore, the strongly enhanced SPs are likely to be concentrated above the metal surface, where the apertures experience severe attenuation of the evanescent field through them leading to the significant contrast and excellent confinement. As indicated by our simulation, features as small as 60 nm on the period of 120 nm can be resolved up to 40 nm below the silver mask using typical resist with contrast  $\sim 0.2$ . In addition, our simulation demonstrates strong transmitted field and tight confinement of the patterned field with scale of a 30 nm aperture size on a 60 nm periodicity [Fig. 3(d)], suggesting the potential of defining even smaller features with silver plasmonic masks. The

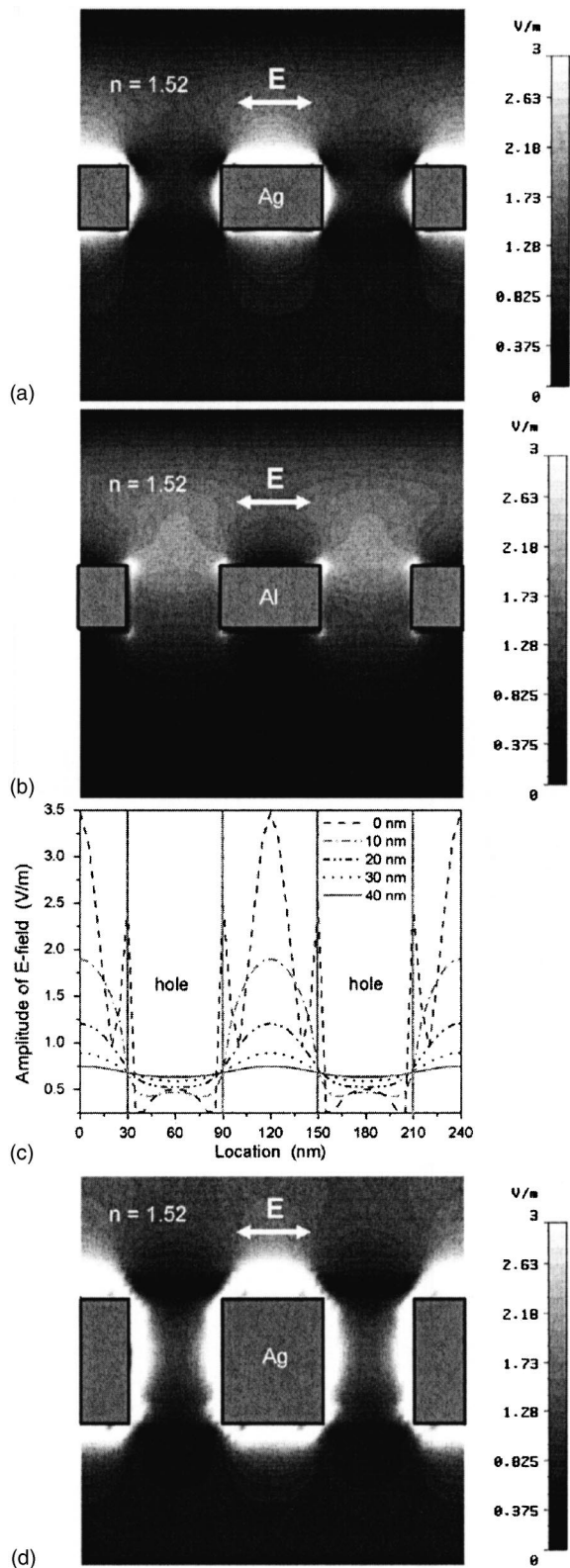


FIG. 3. (a) Simulated amplitude of  $E$ -field at the cross section of Ag hole array; silver film thickness 40 nm, circular hole diameter 60 nm, periodicity 120 nm. (b) Al hole array at the same condition as (a). (c) One-dimensional cross sections of  $E$ -field of the simulation result in (a) as a function of distance  $z$ . (d) Ag hole array; silver film thickness 40 nm, hole diameter 30 nm, periodicity 60 nm.

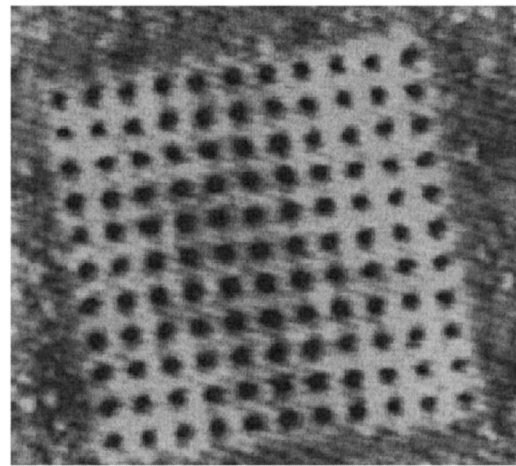


FIG. 4. AFM images of exposure patterns on 200 nm period, where the hole size of 100 nm, silver film thickness of 50 nm, spacer layer thickness of 30 nm, and exposure dose of 80 mJ/cm<sup>2</sup>.

lateral confinement is tight in the case of silver due to the short propagation length ( $<50$  nm) of SPs along the metal surface, therefore the proximity effect for features spaced above 50 nm period is small.

### III. EXPERIMENTAL RESULTS AND DISCUSSION

The configuration of the SP optical lithography is illustrated in Fig. 1. A plasmonic mask designed for lithography at the wavelength of 365 nm (*i*-line) is composed of a silver layer perforated with 2D periodic hole arrays and the silver layer is sandwiched between quartz and poly(methyl methacrylate) (495-PMMA, MicroChem) layers. Quartz and PMMA are selected as the surrounding dielectric materials and their refractive indices are 1.48 and 1.52. As proof of the concept, a negative near-UV photoresist (SU-8) is directly spun on the top of the spacer layer and polymerized on the mask in order to eliminate the gap variation between the mask and the photoresist in the lithography process.

In our lithography experiment, the plasmonic mask is prepared as follows. A variety of dimension of hole arrays are fabricated on 50-nm-thick silver film by focused ion beam (FIB) milling (FIB, FEI Strata 201 XP). Subsequently, a 30-nm-thick spacer layer of PMMA is spun on the top of the patterned silver film, and next the photoresist (SU-8) is spun on the spacer layer. Exposure is performed using a filtered mercury lamp with a radiation peak at 365 nm. After the development, the topography of exposure features is characterized by an atomic force microscope (AFM, Dimension 3100, Digital Instrument).

The AFM image in Fig. 4 is an exposure result obtained from a 200 nm period die. The exposure result shows an exposure pattern on the metal area instead of the hole area which agrees with the simulation result. Features as small as 100 nm have been obtained routinely from the mask with exactly the same dimension. It should be emphasized that the pattern displays a good fidelity to the mask pattern indicating the tight confinement of the optical near-field, by virtue of

the strong localized SPs above the metal area (the feature size does not expand significantly as opposed to the case of aluminum masks). In addition, the height of the exposed resist is  $\sim 15$  nm where no exposed resist is observed outside the hole array, which indicates that the strong field of SPs is only excited on the hole array area. The exposure time in this experiment is only 10 s, corresponding to an exposure dose of  $80 \text{ mJ/cm}^2$  at the mask. Surprisingly, this is comparable to a typical exposure dose used in conventional lithography with larger features. It implies a strong near-field intensity profile, which is in good agreement with simulation result. This method opens up a possibility of high-resolution and high-density nanolithography with superior confinement using a conventional light source, without the complicated setup and vacuum requirement such as in the extreme UV lithography. It is noted that the result at the optimized condition of 60 nm diameter on a 120 nm period has not been verified yet due to the difficulty in the mask fabrication, as silver is easily etched away during the FIB etching process. Currently, we are optimizing the mask fabrication for smaller feature size patterning.

#### IV. CONCLUSIONS

In conclusion, a plasmonic photolithography technique using silver plasmonic masks has been demonstrated. This technique utilizes near-UV light to excite ultrashort wavelengths of SPs on silver thin film to achieve high-resolution lithography. The exposure mechanism utilizes the strong localized SPs coupling between both surfaces of the silver thin film leading to the strong electric field well-confined above the silver area rather than the aperture area. A feature size as small as 100 nm on a 200 nm period has been obtained using an exposure radiation of 365 nm wavelength. Furthermore, our simulation results show a promise of a high-resolution, high-contrast, and well-confined optical lithography, which provides an alternative to nanoimprint process to achieve sub-50 nm lithography.

#### ACKNOWLEDGMENTS

The authors are grateful to Fujino Makoto, Zhaowei Liu, and Dongmin Wu for helpful discussions. This work was supported by MURI (Grant No. N00014-01-1-0803), NSF on Nanoscale Science and Engineering Center (NSEC) (Grant No. DMI-0327077), and NSF (Grant No. DMI-0218273).

- <sup>1</sup>M. M. Alkaisi, R. J. Blaikie, and S. J. Mcnab, *Microelectron. Eng.* **53**, 237 (2000).
- <sup>2</sup>J. G. Goodberlet and H. Kavak, *Appl. Phys. Lett.* **81**, 1315 (2002).
- <sup>3</sup>R. R. Kunz, M. Rothschild, and M. S. Yeung, *J. Vac. Sci. Technol. B* **21**, 78 (2003).
- <sup>4</sup>H. Schmid, H. Biebuyck, B. Michel, and O. J. F. Martin, *Appl. Phys. Lett.* **72**, 2379 (1998).
- <sup>5</sup>R. S. Dhaliwal *et al.*, *IBM J. Res. Dev.* **45**, 615 (2001).
- <sup>6</sup>S. Y. Chou, P. R. Krauss, and P. J. Renstrom, *Science* **272**, 85 (1996).
- <sup>7</sup>M. Colburn, T. Bailey, B. J. Choi, J. G. Ekerdt, S. V. Sreenivasan, and C. G. Willson, *Solid State Technol.* **44**, 67 (2001).
- <sup>8</sup>M. C. McAlpine, R. S. Friedman, and C. M. Lieber, *Nano Lett.* **3**, 443 (2003).
- <sup>9</sup>E. B. Cooper, S. R. Manalis, H. Fang, H. Dai, K. Matsumoto, S. C. Minne, T. Hunt, and C. F. Quate, *Appl. Phys. Lett.* **75**, 3566 (1999).
- <sup>10</sup>X. Yin, N. Fang, X. Zhang, I. B. Martini, and B. J. Schwartz, *Appl. Phys. Lett.* **81**, 3663 (2002).
- <sup>11</sup>R. D. Piner, J. Zhu, F. Xu, S. Hong and C. A. Mirkin, *Science* **283**, 661 (1999).
- <sup>12</sup>H. Zhang, S.-W. Chung and C. A. Mirkin, *Nano Lett.* **3**, 43 (2003).
- <sup>13</sup>W. Srituravanich, N. Fang, C. Sun, Q. Luo, and X. Zhang, *Nano Lett.* **4**, 1085 (2004).
- <sup>14</sup>W. L. Barnes, A. Dereux, and T. W. Ebbesen, *Nature (London)* **424**, 824 (2003).
- <sup>15</sup>T. W. Ebbesen, H. J. Lezec, H. F. Ghaemi, T. Thio, and P. A. Wolff, *Nature (London)* **391**, 667 (1998).
- <sup>16</sup>T. Thio, H. F. Ghaemi, H. J. Lezec, P. A. Wolff, and T. W. Ebbesen, *J. Opt. Soc. Am. B* **16**, 1743 (1999).
- <sup>17</sup>A. Krishnan, T. Thio, T. J. Kim, H. J. Lezec, T. W. Ebbesen, P. A. Wolff, J. Pendry, L. Martin-Moreno, and F. J. Garcia-Vidal, *Opt. Commun.* **200**, 1 (2001).
- <sup>18</sup>A. Dogariu, A. Nahata, R. A. Linke, L. J. Wang, and R. Trebino, *Appl. Phys. B: Lasers Opt.* **74**, S69 (2002).
- <sup>19</sup>L. Salomon, F. Grillot, A. V. Zayats, and F. V. de Fornel, *Phys. Rev. Lett.* **86**, 1110 (2001).
- <sup>20</sup>H. Raether, *Surface Plasmons on Smooth and Rough Surfaces and on Gratings* (Springer, Heidelberg, 1988), pp. 25–30.
- <sup>21</sup>J. H. Weaver and H. P. R. Frederkse, *CRC Handbook of Chemistry and Physics*, 83rd ed. (CRC Press, Boca Raton, FL, 2002), Sec. 12, pp. 133–156.